

Prediction of mechanical stresses of single rotor blade of low pressure of Nasiriya power plant steam turbine

Noura A.Essi¹, Rafid M. Hunnun², Hazim I. Radhi³

¹ Department of Mechanical Engineer, College of Engineering, Thi-Qar University, Iraq

² Department of Mechanical Engineer, College of Engineering, Thi-Qar University, Iraq

³ Department of Mechanical Engineer, College of Engineering, Thi-Qar University, Iraq

Abstract

In this paper, two types of stresses acting on the single rotor blade of low pressure steam turbine for Nasiriya power plant were studied. The first type of stresses was the stresses due to pressure force on the single rotor blade, while the second type of stresses are the centrifugal stresses. The stresses due the pressure force were studied in this paper at three loads (70, 140, 210 MW), while the pressures acting on the first rotor blade of steam turbine were 512, 3311.7, 6496.8 Pa respectively. In addition, the blade was fixed at the root and free at the end, while the rotational speed of blade was 341 rad/sec was applied as rotational load. The results showed that the rotational load has the greatest effect on the blade. Also the stresses due to rotational load are higher than stresses due to steam pressure at the three loads.

Keywords: Steam turbine, rotational load, steam pressure.

1.Introduction

Blades could be considered as the turbine's heart, due to the fact that they're the main elements converting the working fluid energy to kinetic energy. The turbine's effectiveness and reliability are dependent on the suitable blade design. Thus, it is very important for engineers that are involved in the turbine design to overview the necessity and basic engineering aspects of the steam turbine blades, which is a multi-disciplinary job. It is involved with the disciplines of thermo-dynamic, aero-dynamic, mechanic and material science [1]. There are various types of blades that may be classified according to their implementations to the three turbine modules which are: high-pressure turbine, intermediate-pressure turbine and low-pressure turbine. The first two types, high-pressure and intermediate-pressure, are identifies by high temperatures and the fact of them containing small blades which have to maintain small centrifuge forces [2]. Low-pressure turbine blades, designed for the extraction of the final energy remainder from the passing steam flow, are rather large scale rotating air-foils because of the considerable centrifuge forces that are experienced

throughout ordinary operations. Statistics show that low-pressure turbine blades are usually more susceptible to failure than those of the high pressure turbine and intermediate pressure turbine [1].

There are typical metals used in the manufacture of steam turbine blades [3]:

1. Stainless steel 403: is essentially the industry's standard blade material and, on impulse steam turbines, it is probably found on over 90 percent of all the stages. It is used because of its high yield strength, endurance limit, ductility, toughness, erosion and corrosion resistance, and damping.
2. Stainless steel 422: is applied only on high temperature stages (between 371 and 482 °C), where its higher yield, endurance, creep and rupture strengths are needed.
3. Super alloys used in the second quarter of the twentieth century at high temperatures and divided into:

- a. Nickel-base super alloys.
 - b. Cobalt-base super alloys: are called Haynes Satellite Alloy.
 - c. Iron-base super alloys.
4. Titanium : Its high strength, low density, and good erosion resistance make it a good candidate for high speed or long-last stage blading.

There are many of research analysis the stresses on the blades of turbine where Arkan (2008) [4] studied the stresses on the low-pressure steam turbine rotor blade. He investigated effect of cross section area on the centrifugal stress by using three cross section area of blade

- a- Constant cross sectional area.
- b- Variable cross sectional area.
- c- Variable cross sectional area and the cross sectional area less than in case b.

In all cases observed the centrifugal force decreases with the height of the blade. The centrifugal force and stresses in case **a** are large with compared to the variable cross sectional area blades in both cases (**b** and **c**), where use of variable cross sectional areas leads to reduce the centrifugal force and the centrifugal stress. The bending stress was greater for variable cross sectional area blades when compared with straight blades.

Amr and Liang (2012) [5] investigated the stress distribution of a turbopump turbine by using finite element analysis. CAD software was used to modeling geometry of a group of blades and a sector of the disc and exported to a ANSYS package for analysis. They used six kinds of loads (rotational load, gas pressure load, shrink-fitted load, all the mechanical loads rotation, gas pressure and shrink-fitted, temperature gradient as a thermal load and combining mechanical and thermal). They found the

thermal stress had greatest effect on the disc while it was not significant on the blade. In addition, the maximum stresses in the blades were observed to be induced by the rotational and thermal loads rather than the gas pressure load.

Vaishaly and Ramarao (2013) [6] analyzed the steady state stress on the last stage of low pressure steam turbine blade. They used various loads such as pressure load and centrifugal load to predict this study. ANSYS package driven by customized software and the pressure distribution is mapped on the blade surface. They observed from their results the peak radial stress distribution at the root lug locations where the peak stress values is around 1680 MPa, also they found the peak axial stress values was around 900 MPa at root lug locations. In addition, It was found that the stresses at those locations were lesser than the allowable stress.

Ali and Abdullah (2013) [7] studied the stresses at the last stage blades in Baji thermal power plant station. In their study two cases were studied which the blades without lacing rod and blades with lacing rod. ANSYS 12.1 was used to obtain different stresses in two case were studied. They concluded that the centrifugal force is greater at the root and less at tip of the blade due to the cross section area is as large as possible at the root of blade. In addition, the stresses due to centrifugal force is greater than the stresses of pressure force acting on the blade. Also the stresses in case the blade with lacing rod were less than stresses in cases without lacing rod.

In this work, the two types of mechanical stresses on the first rotor blade of low pressure steam turbine for Nasiriya power plant were studied.

2. Model description

In this paper, calculate the stress distribution of single rotor blade for Nasiriya power plant, due to the

complex shape of the blade, the change of the blade area , the curvature angle of blade were taken of the real blade at the station and then the blade was modeled by AutoCAD indicated in Fig. 1 and use ANSYS 15.0 software to calculate stress distribution of blade.

The material of blade was X20Cr13 grade 1.4021 , with thermal and mechanical properties are indicated in table 1 and chemical composition of this material of blades is indicated in table 2 and 3 respectively [8].

In this paper, three of steam pressures were used with each load as indicated in table 3. Also the rotational speed for blade was 341 rad/sec.

Table -1: Mechanical and thermal properties of blade material[8].

Density (kg.m ³)	7700
Modulus of elasticity (GPa)	205
Specific heat (J/kg.K)	460
Thermal conductivity (W/m.K)	30
Electrical resistivity (Ω.mm ² /m)	0.6
Tensile strength (MPa)	550
Ultimate strength (MPa)	880
Modulus shear (GPa)	76
Elongation A%	15

Table- 2: Chemical composition of material blade [8].

C	Si	Mn	P	S	Cr
0.16-0.25	<1	< 1.5	< 0.04	< 0.015	12-14

Table -3: Boundary condition of blade.

Loads (MW)	Velocity (m/s)	Pressure (Pa)
70	200	512
140	275	3311.7
210	350	6496.8

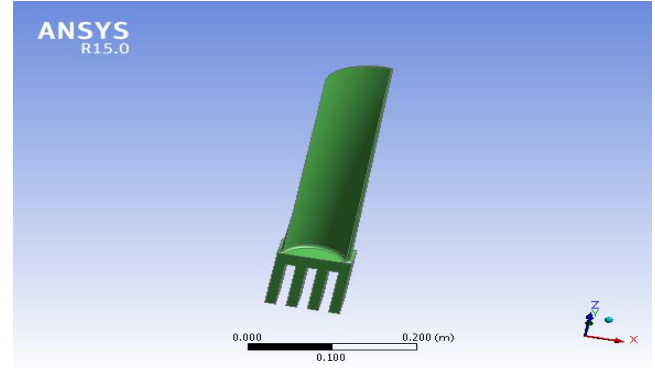


Fig. 1: First rotor blade.

3.Mathematical model

The principle stresses (maximum and minimum stresses) on inclined planes are [9][10]:

$$\sigma_1 = \frac{1}{2}(\sigma_x + \sigma_y) + \frac{1}{2}\sqrt{[(\sigma_x - \sigma_y)^2 + 4\tau_{xy}^2]} \quad (1)$$

$$\sigma_2 = \frac{1}{2}(\sigma_x + \sigma_y) - \frac{1}{2}\sqrt{[(\sigma_x - \sigma_y)^2 + 4\tau_{xy}^2]} \quad (2)$$

The maximum shear stress is :

$$\sigma_{max} = \frac{1}{2}\sqrt{[(\sigma_x - \sigma_y)^2 + 4\tau_{xy}^2]} = \frac{1}{2}(\sigma_1 - \sigma_2) \quad (3)$$

3.2 Stresses in Rotor blades

The stresses acting on a rotating turbine blade are[4]:

1. Centrifugal stress due to rotation.
2. Bending stress due to the fluid pressure and change of momentum.
3. Total stresses.

3.2.1 Centrifugal stress

3.2.2 The centrifugal stresses

The centrifugal stresses at the blade section are the centrifugal force in that section divided by the area of the blade section, and can be written as [4]:

$$\sigma_{cf}(x) = \frac{F_{cf}(x)}{A(x)} \quad (4)$$

The general equation for centrifugal force is :

$$F_{cf} = mr\omega^2 \quad (5)$$

When taken an infinitesimal element (dz) is separated in section Z as shown in figure 2 the centrifugal force developed by this element during disc will be [4]:

$$df_{cf} = dm \cdot \omega^2 (R_r + z) \quad (6)$$

$$dm = \rho \cdot A(z) dz \quad (7)$$

$$df_{cf} = \rho \cdot \omega^2 \cdot A(z) \cdot (R_r + Z) dz \quad (8)$$

$$F_{cf}(X) = \int_x^{lb} \rho \cdot \omega^2 \cdot A(z) \cdot (R_r + Z) dz \quad (9)$$

Consider the blade as cantilever beam with variable cross-section and fixed at the root so that the cross section variable according to the equation:

$$\left(\frac{A(z)}{A_r}\right)^{lb} = \left(\frac{At}{Ar}\right)^z \quad (10)$$

$$\frac{A(z)}{Ar} = \left(\frac{At}{Ar}\right)^{z/lb} \quad (11)$$

$$A(z) = Ar \cdot \left(\frac{At}{Ar}\right)^{z/lb} \quad (12)$$

$$F_{cf} = \rho \cdot \omega^2 \int_x^{lb} \left[Ar \cdot \left(\frac{At}{Ar}\right)^{\frac{z}{lb}} \right] \cdot (R_r + Z) dz \quad (13)$$

$$F_{cf} = \rho \cdot \omega^2 \left[R_r \int_x^{lb} Ar \cdot \left(\frac{At}{Ar}\right)^{\frac{z}{lb}} \cdot dz + \int_x^{lb} Ar \cdot z \left(\frac{At}{Ar}\right)^{\frac{z}{lb}} \cdot dz \right] \quad (14)$$

After solving and finding the integral equation (14) it gets the centrifugal force at any point along the length of blade as in equation (15)

$$F_{cf}(X) = \rho \cdot \omega^2 \left[\frac{Ar \cdot \left(\frac{At}{Ar}\right)^{\frac{z}{lb}} \cdot R_r \cdot Lb}{\ln\left(\frac{At}{Ar}\right)} + \frac{Ar \cdot \left(\frac{At}{Ar}\right)^{\frac{z}{lb}} \cdot z \cdot Lb}{\ln\left(\frac{At}{Ar}\right)} - \frac{Ar \cdot \left(\frac{At}{Ar}\right)^{\frac{z}{lb}} \cdot Lb^2}{\left[\ln\left(\frac{At}{Ar}\right)\right]^2} \right]_x^{Lb} \quad (15)$$

Where (F_{cf} , At , Ar , R_r , Lb , ρ) represent the centrifugal force, cross section area of blade tip, cross section area of blade root, radius from shaft center at the blade root, blade height and material density respectively.

3.2.2 The bending stress

The moving blade suffers from the bending force in addition to the centrifugal force. The bending force exerted by the working fluid on the moving blade is essentially distributed load [11].

The blade without lacing rod can be regarded as a cantilever beam of a variable cross-section area which is stressed by a distributed load ($q(x)$)

as shown in Fig.(3) The components of aerodynamic force (q), is the axial force (qa) and the tangential force (qw) shown in Fig.(3) this force produces bending stress on the blade.

The bending moment effect is on the level of the main axes of inertia (u, v) as shown Fig.(3). The axial force [11]:

$$qa = \rho_f \cdot cf_3 (Vw_2 - Vw_3) \quad (16)$$

The tangential force [11]:

$$qw = \rho_f \cdot cf_3 \cdot (cf_2 - cf_3) + (p_2 - p_3) \cdot s \quad (17)$$

Or, when the axial velocity is constant $cf_2 = cf_3$, then

The tangential force:

$$qw = (p_2 - p_3) \cdot s \quad (18)$$

The resultant force is:

$$q = \sqrt{qw^2 + qa^2} \quad (19)$$

where, the component force on the main axes (U, V):

The force for the axis (U):

$$qu = q \cdot \sin(Q) \quad (20)$$

The force for the axis (V):

$$qv = q \cdot \cos(Q) \quad (21)$$

But Q is the angle between the force on the axis (v) and the result force shown Fig.(3), then:

$$Q = b + st \quad (22)$$

$$b = \tan^{-1} \frac{qa}{qw} \quad (23)$$

$$st = \left[\tan^{-1} \left[\frac{-I_{xy}}{I_x - I_y} \right] \right] \cdot 2 \quad (24)$$

he bending moment about axes (V, U) at any section of the blade height is:

$$Mv = \int_x^{Lb} qv(z) \cdot (z - x) dz \quad (25)$$

$$Mu = \int_x^{Lb} qu(z) \cdot (z - x) dz \quad (26)$$

The bending stress will be calculated for the following points in which the stress is maximum as shown in Fig.(3).

For the entrance or leading edge of the blade, the stress is:

$$\sigma_{b1} = \frac{Mv_1 \cdot vv_1}{I_u} + \frac{Mu_1 \cdot uu_1}{I_v} \quad (27)$$

While for the exit or trailing edge:

$$\sigma_{b2} = \frac{M_{v2} * vv2}{I_u} + \frac{M_{u2} * uu2}{I_v} \quad (28)$$

And for a point located at the intersection of the v axis and the back of the blade which of course is subjected to compression stresses is:

$$\sigma_{b3} = - \frac{Mv * vv3}{I_u} \quad (29)$$

where, the negative sign is for compression.

3.2.3 Total stress

The total stress at a given point on a turbine blade may be found by adding the centrifugal stress at that point to the bending stress.

The equation of total stresses is :

$$\sigma_t = \sigma_{cf} + \sigma_b \quad (30)$$

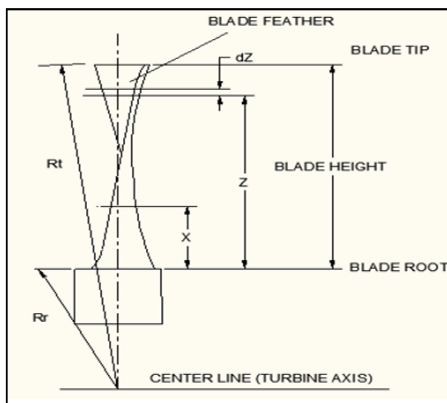


Fig. 2 :The calculation of the centrifugal force [4].

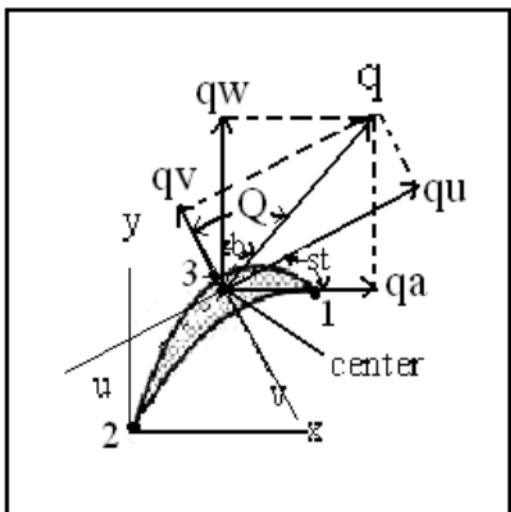


Fig. 3: Cross section of single rotor blade[12].

4. Results and discussion

Fig. 4 shows the contour of distribution for Von Mises stresses through the single rotor blade at load 70 MW. The pressure applied on the blade is 512 Pa. It can be observed from this figure the maximum stresses occurs at the leading edge of root blade, the value is 3.141 MPa. In addition, it can be notice the minimum stress occurs at the tip of blade, where this value is 0.3498 MPa. The reason that the bending moment is large at the root of the blade, then it decreased when mover towards of the end of blade, therefore the stresses resulting from steam force are high at the root of the blade because their value depends on the bending.

Fig. 5 indicates the contour of equivalent stress distribution on the first rotor blade at load 140 MW. The pressure applied at this load is 3311.7 Pa. It can be seen from this figure the maximum stresses is larger than maximum stress at load 70 MW, the maximum stress at this load is 20.32 MPa. The reason that the increase in the steam pressure on the blade leads to increase the stress on the blade, also from this figure can be observed that the stresses are constructed on the leading edge of the root due to bending moment is large at this region, the stresses is decreased whenever headed to tip of blade where the value of minimum stress that occur at the tip of blade 2.257 MPa. Additionally, the stresses acting on the blade do not access permissible stress of blade.

Fig. 6 describes the distribution of von mises stresses on the rotor blade at maximum load (210 MW) where the pressure applied is 6496.8 Pa. It can be noted that the maximum stresses occurs at leading edge of the root blade and minimum stresses at tip of blade. The value of maximum stresses is 39.866 MPa and minimum stress is 4.4295 MPa. Also it can be observed the maximum stress at this load is larger than maximum stresses at loads (70, 140 MW). The reasons that construction of stresses on leading edge of blade is the bending on the root of blade is larger than moment in the tip of blade. also the increasing in the flow rate at maximum load causes increasing the pressure force acting on the blade and the therefore increasing the stresses acting on the blade.

Fig. 7 shows the Von Mises stresses due to the effect of centrifugal force acting on the blade. It can be seen

from this figure the maximum stresses occurs at the leading edge and trailing edge near of the root blade. The value of maximum stresses is 51.346 MPa and the stresses are reduced when move towards the upper end of blade until reaches to minimum stresses at the tip of blade is 5.705 MPa. The reason that the centrifugal force is as large as possible at the root and decreases as we move towards upper end of the blade. The centrifugal force is function to the length of the blade as shown in equation 15. Where the centrifugal force is variable according to mass and length of the blade. In addition, the stresses results at centrifugal force larger than the stresses due to the steam pressure at all loads are studied.

Table 4 represents the results of maximum and minimum Von Mises stresses on the blade due to the steam pressure on the blade at three loads (70, 140, 210 MW) and the stresses due to the centrifugal force.

From the results of this table, we observe the rotational load has the greatest effect on the blade. Also the stresses due to rotational load is higher than stresses due to steam pressure at the three loads.

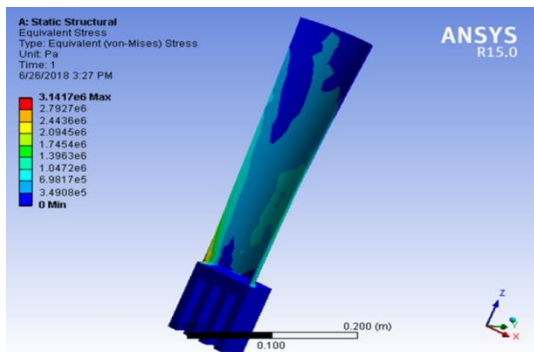


Fig.4 Von Mises stresses on the blade at 70 MW

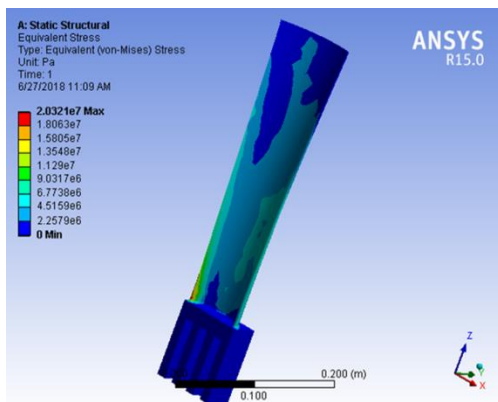


Fig. 5 Von Mises stresses on the blade at 140 MW

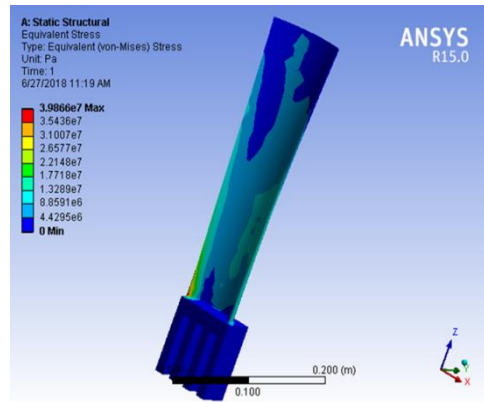


Fig. 6 Von Mises stresses on the blade at 210 MW

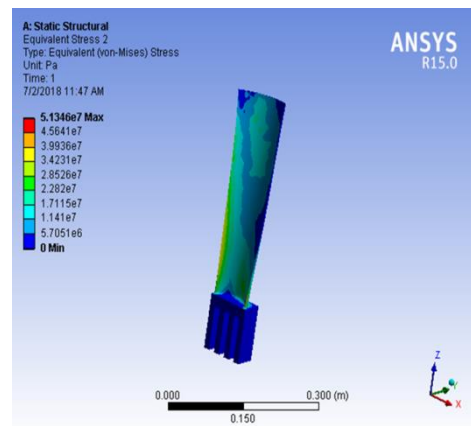


Fig. 7 Von Mises stress due to the centrifugal force

Table- 4 : Results of Von Mises stresses on the blade at different loads.

Type of loads	Maximum stresses (MPa)	Minimum stresses (MPa)
Pressure load at 70 MW	3.1417	0.34908
Pressure load at 140 MW	20.321	2.2579
Pressure load at 140 MW	39.866	4.4295
Centrifugal load (341 rad/sec)	51.346	5.7051

5. Validation

To check the validity of stress analysis, a verification was made by solving theoretical mode of Alaa Mohammed Abdullah [7].

Alaa analyzed the stresses of steam turbine blades at the last stage in beji thermal power station. The pressure force are applied as boundary condition is 2318.7 Pa and value of angular velocity for blade is 341 rad/sec.

The materials of blades were X15Cr13, the boundary conditions were applied is the same.

Fig. 8 shows the comparison between the numerical results of present model with simulation results of Alaa's model [7]. From this figure it can be notice that, the agreement between the simulation results of the present model with the simulation results of Alaa's model [7] is acceptable with the average error of 6.78 %.

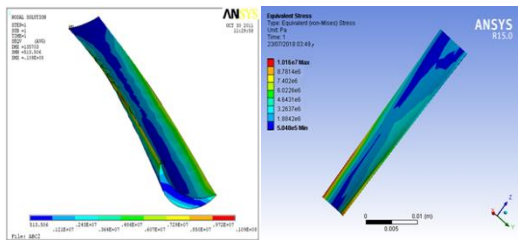


Fig. 8 Von Mises stresses contours as comparison between present model and Alaa 's model [7]

6. Conclusion

1. The distribution of Von Mises stresses due to the pressure of steam was concentrated on the leading edge and trailing edge of the blade.
2. The stresses generated on the blade due to centrifugal force was concentrated on the leading edge and trailing edge in the root blade.
3. The stresses generated due to the centrifugal force was larger than the stresses generated due to pressure force.

Nomenclature

F_{st} : steam force (N).

F_{cf} : centrifugal force (N).

m : mass of blade (kg).

A_t : cross section of blade At tip (m^2).

A_r : cross section of blade at tip (m^2).

σ : normal stress (Pa).

τ : shear stress (Pa).

τ_{max} : maximum shear stress (Pa)

τ_ϕ : shear stress on the inclined plane (Pa).

σ_ϕ : normal stress on the inclined plane (Pa).

V_{w2} : velocity of whirl at exit of moving blade.

V_{w1} : velocity of whirl at the entrance of moving blade.

ω : rotational speed of turbine (rpm).

I_v, I_u = Moments of inertia of axis vv and uu .

$\sigma_{b1}, \sigma_{b2}, \sigma_{b3}$ = Bending stresses in point 1, 2, 3.

$vv1, vv2, vv3$ = Destines from the axis u and the point 1, 2, 3.

$uu1, uu2, uu3$ = Destines from the axis v and the point 1, 2, 3.

p_2, p_3 = Pressure inlet and outlet of moving blade.

s = Spacing or pitch from two moving blade.

References

- [1] Reddy, A.S., Ahmed, M.I., Kumar, T.S., Reddy, A.V.K. and Bharathi, V.P., (2014). Analysis Of Steam Turbines. International Refereed Journal of Engineering and Science, (Vol. 3, No.2, pp.32-48).
- [2] Heidari, M., & Amini, K. (2017, May). Structural modification of a steam turbine blade. In *IOP Conference Series: Materials Science and Engineering* (Vol. 203, No. 1, p. 012007). IOP Publishing.

- [3] Wang, W. Z., Xuan, F. Z., Zhu, K. L., & Tu, S. T. (2007). Failure analysis of the final stage blade in steam turbine. *Engineering Failure Analysis*, 14(4), 632-641.
- [4] Al-Taie, A. K. H. (2008). Stress Evaluation of Low Pressure Steam Turbine Rotor bBlade and Design of Reduced Stress Blade. *Engineering and Technology Journal*, 26(2), 169-179.
- [5] Amr, E., & Liang, G. Z. (2012). Stress of a Rocket Turbine under Different Loads Using Finite Element Modeling. In *Applied Mechanics and Materials* (Vol. 232, pp. 691-696). Trans Tech Publications.
- [6] Vaishaly, P. and Ramarao, B.S.V., (2013). Finite element stress analysis of a typical steam turbine blade. *International Journal of Science and Research*. 4(7).
- [7] Ali D.S.M. J and Abdullah Alaa M., (2013). Stress analysis of steam turbine blades at the last stage in Beji thermal power plant. *Al rafidian Engineering* .21(3).
- [8] EN, D., (2005). Stainless steels-Part 1: List of Stainless Steels. British Standards Institution.
- [9] Heran, E. J.(1997). *Mechanics of Materials 1: An Introduction to the Mechanics of Elastic and Plastic Deformation Solids and Structural Materials*. Butterworth-Heine-mann, London.
- [10] Tahir H. T. (2004). *Mechanical Design of Moldboard Plow Bottom Throe Stresses Analysis and Performance Measurement*. PhD Thesis, University of Mosul.
- [11] Alwan, R. A., AbdulRazzaq, A., & Al-Taie, A. K. H. (2007). Design of a Constant Stress Steam Turbine Rotor Blade. *Journal of Engineering and Sustainable Development*, 11(3), 76-94.